Maladaptation of Memory Systems Impairs Dorsal CA1-Dependent Temporal Binding and Declarative Memory in The *Cntnap2* Knockout Mouse Model of Autism

Elise C Rawlinson[1], Michael H. McCullough[1,2], Aline Marighetto[3,4], A. Shaam Al Abed[1,5*#], Nathalie Dehorter[1,5*#]

Abstract 166

The CA1 region of the hippocampus plays a multifaceted role in cognitive functions related to temporal binding, spatial navigation, and social interactions. Growing evidence reports a role of the hippocampus in the pathophysiology of autism spectrum disorder, particularly in social interactions and cognitive domains. Yet, the mechanisms driving hippocampal-driven cognitive impairments remain poorly defined. Here, we characterized how dorsal CA1 dysfunction impacts the long term retention of temporally discontiguous events. We found that *Cntnap2* knockout mice exhibit reduced temporal binding capabilities compared to controls, stemming from decreased dorsal CA1 activity during temporal gaps. We further demonstrate a deficit of the flexibility component of relational/declarative memory in *Cntnap2* KO mice. This impairment was secondary to the use of a procedural learning strategy associated with the imbalance of memory systems, in favor of the activity of the frontal-striatal areas, instead of the hippocampus. This study offers deeper insights into how memory systems are mistuned in autism, opening new avenues for understanding and addressing atypical cognition in this condition.

Affiliations:

[1] Eccles Institute of Neuroscience, John Curtin School of Medical Research, The Australian National University, Canberra, ACT, Australia

[2] School of Computing, College of Engineering, Computing and Cybernetics, The Australian National University

[3] Neurocentre Magendie, Physiopathologie de la plasticité neuronale, U1215, INSERM, F-33000 Bordeaux, France

[4] Université de Bordeaux, F-33000 Bordeaux, France.

[5] The Queensland Brain Institute, The University of Queensland, Brisbane, QLD, Australia

* These authors contributed equally to the work and are listed alphabetically

[#] Co-corresponding authors: A. S. Al Abed (shaam.alabed@anu.edu.au) and N. Dehorter

(n.dehorter@uq.edu.au), The Australian National University and The University of Queensland.

Key words: Autism, episodic memory, hippocampus, CA1

Abbreviations: ASD: Autism Spectrum Disorder; KO: Knock-Out;

Introduction

Autism spectrum disorder (ASD) is a lifelong neurodevelopmental disorder comprising difficulties in social behavior, atypical communication skills, and the presence of restricted or repetitive behaviors or interests (DSM-5 & Association American Psychiatric, 2013). Beyond these core features, individuals with ASD present with difficulties in cognitive domains. In particular, people with ASD present with atypicalities in episodic/declarative memory, the ability to recall specific events and experiences, which can impact daily functioning and adaptability (Bal et al., 2015). Yet, the underlying neurological mechanisms of these cognitive impairments remain to be fully elucidated.

The integrity of relational memory representations is altered in ASD (Minor et al., 2023). We demonstrated that the long-term retention of typical relational/declarative memory required temporal binding capacities (Sellami et al., 2017). Therefore, we hypothesized that temporal binding could be reduced in ASD, leading to altered episodic memory. The hippocampus plays a critical role in episodic memory formation and maintenance (Eichenbaum, 2004). In particular, the CA1 region of the hippocampus is essential for integrating temporal information and creating a cohesive sense of time (Eichenbaum, 2014; Sellami et al., 2017). Disruptions in this function affect the ability to sequence events and develop temporal relationships, which are often impaired in individuals with ASD (Maister & Plaisted-Grant, 2011; Vogel et al., 2022). While most research in autism has focused on the dysregulation of the prefrontal cortex and the basal ganglia, recent studies have highlighted that hippocampal disruption are key in the pathophysiology of ASD (Banker et al.,2021) Yet, how hippocampal subfield activity, such as the dorsal CA1 (dCA1), drives episodic memory atypicalities in ASD is currently unknown.

Here, we aimed to dissect declarative memory atypicality and the role of the dCA1-dependent processing in related cognitive deficits in ASD. We used the *Cntnap2* knock out (KO) mouse model of ASD, that exhibits autism-like phenotypes, including social behavior deficits, hyperactivity, and seizures (Peñagarikano et al., 2011; Peñagarikano & Geschwind, 2012). We demonstrate that *Cntnap2* KO mice present with reduction of temporal binding capabilities and dCA1 activation during temporal binding-dependent memory tasks, which support deficits in declarative memory.

Results

Cntnap2 KO mice demonstrate reduced temporal binding capability.

The capacity to bridge temporally distant events, called temporal binding, is critical to enable declarative memory formation (Sellami et al., 2017). To test this elemental process, we tested *Cntnap2* KO mouse model in the trace fear conditioning paradigm (TFC; **Fig. 1A**). In this paradigm, mice are required to associate a tone (Conditioned Stimulus) with a mild electric foot-shock (Unconditioned Stimulus), separated by a time interval (i.e. Trace, (Sellami et al., 2017)). In the first step, the conditioning, independent groups of mice were exposed to three tone-shock pairings separated by time intervals between 5 and 60 sec (*i.e.* T5, T20, T40, and T60; **Fig. 1A**). 24h later, efficient temporal binding was assessed by re-exposing the animal first to the conditioning *tone* in a neutral context (*i.e.* tone test) and second to the conditioning *context* alone, which evaluates contextual memory. Efficient temporal binding capacity is illustrated by the animal's capacity to freeze (Blanchard et al., 1986) when re-exposed to the conditioning tone in a neutral context. As previously demonstrated (Al Abed, Sellami, et al., 2020; Sellami et al., 2017), control mice displayed efficient temporal binding capacity up to a 40 sec trace interval (**Fig. 1C**), illustrated by strong and specific fear of the tone (**Fig. 1C**). Interestingly, *Cntnap2* KO mice displayed a strong and specific freezing to the tone for up to a 20 sec trace interval (**Fig. 1C**, T20), but not for 40 sec (**Fig. 1C**, T40), indicating reduced temporal binding capacity compared to control mice. A precise memory includes the ability to distinguish between two contexts: conditioning context and neutral context. As the duration of the trace interval increases, the mouse's ability to differentiate between the two contexts diminishes (Sellami et al., 2017). While WT mice showed specific context discrimination up to a 40 s trace interval, *Cntnap2* KO mice presented with lower context discrimination (**Fig. 1D**). Taken together, our results demonstrate that *Cntnap2* KO mice display reduced contextual discrimination secondary to reduced temporal binding capacity.

Mistuning of dorsal CA1 activity during temporal binding in *Cntnap2* KO mice

The sustained activity of the dCA1 during the trace interval allows to bridge two temporally distant events in memory (Huerta et al., 2000; Sellami et al., 2017). Whilst alterations in item binding have already been reported, the underlying mechanisms have not been described in ASD (Minor et al., 2023). To dissect dCA1 activity during temporal binding in *Cntnap2* KO mice, we recorded calcium transients during encoding and recall of trace fear conditioning, using fiber photometry in animals trained under the 40s-trace interval (**Fig. 2A, B**). As in figure 1, both WT and *Cntnap2* KO mice implanted with an optic fiber could associate the tone and the shock, reaching a high level of freezing after 3 tone-shock pairings (**Fig. 2C**). While the

frequency of the calcium transients did not differ between WT and C*ntnap2* KO mice throughout conditioning, their amplitude was significantly reduced during the presentation of the second tone and consistently across the 3 trace intervals in *Cntnap2* KO mice (**Fig. 2D**). These results suggest a lack of synchronized neuronal activity, as previously reported (Simon & Wallace, 2016). They also show that the sustained activity of dCA1 pyramidal cells during the trace interval in WT mice is required for efficient temporal binding, enabling adequate association, *which is not present in Cntnap2 KO mice*.

In the tone test, as in Fig. 1C, *Cntnap2* KO mice displayed an impaired recall of the trace fear memory, characterized by lower freezing to the tone compared WT mice (**Fig. 2F**). While the frequency of calcium transient remained unchanged, the amplitude of the peaks was lower during the tone presentation and the subsequent trace period in *Cntnap2* KO compared to WT mice. Further dissection of calcium activity during the tone test showed a large transient 6 seconds after the tone onset in the WT mice (**Fig. 2I**). It is likely that this neuronal activity reflects the integration of the freezing sensory feedback, leading to sustain freezing during the tone presentation. In contrast, the freezing behavior in the *Cntnap2* KO mice did not lead to an increase in dCA1 activity, indicating an absence of sensory integration and lack of encoding which ultimately prevent recall.

During the trace period of the tone test, *Cntnap2* KO mice also displayed significantly lower activity (**Fig. 2J**), compared to WT mice. This result further confirmed that the reduction of temporal binding capacity in *Cntnap2* KO mice stems from a lack of sustained dCA1 activity during encoding and recall of the tone-shock association.

Egocentric learning and inflexible long-term memory in *Cntnap2* KO mice

Long-term retention of declarative memory requires temporal binding to compare and combine temporal distant pieces of information (Eichenbaum, 2017). Following the observation that *Cntnap2* KO mice present with reduced temporal binding capabilities, we aimed to dissect declarative memory atypicalities in ASD. We utilized a unique radial task in mice, assessing the qualitative alterations of declarative memory (Etchamendy et al., 2012; Marighetto et al., 1999). In rodents, declarative memory can be reduced to its main function of relating what happened, when, and where (Cohen et al., 1997), and is referred to as Relational/Declarative memory (R/DM; Al Abed, Sellami, et al., 2020; Etchamendy et al., 2012; Marighetto et al., 2011, 1999; Mingaud et al., 2007; Sellami et al., 2017). The R/DM task is divided into two stages: acquisition and flexibility test (**Fig. 3A**). In the acquisition stage, mice are trained to explore 3 pairs of adjacent arms. Within each pair, only one arm contained a food reward, which remains in the same location throughout the task. 24h after reaching the learning

criterion (see Methods), the flexibility of the memory learnt during acquisition was probed by recombining 2 pairs, without changing the position of the reward (pairs A and B recombined into Pair AB; **Fig. 3A**). Both wild-type (WT) and *Cntnap2* KO mice were able to acquire the task (**Fig. 3B**). *Cntnap2* KO mice tended to take more days (**Fig. 3C**) and reached higher levels of performance on the last of training (**Fig. 3B**, right panel). In the flexibility test, their performance dropped significantly between the last training session and the flexibility test (stage 2 of the R/DM task), but *Cntnap2* KO mice also performed significantly lower than WT in the test (**Fig. 3C**). In contrast, both groups performed similarly on the control pairs: unchanged pair C, with high performance **(Fig. 3D)**, and the new pair N, at chance levels **(Fig. 3E).** How can we explain the lack of flexibility? We have previously shown that the flexibility component of R/DM depends on the learning strategy used during the acquisition stage: spatial or procedural, the latter requiring repetition and lateralization (Mingaud et al., 2007; Sellami et al., 2017). Therefore, the chance-level flexibility performance of *Cntnap2* KO mice suggests a bias towards an egocentric learning strategy, in line with the well-documented prominence of behavioral inflexibility in ASD (Uddin et al., 2015). This was confirmed by analyzing the left/right lateralization during acquisition. *Cntnap2* KO mice displayed significantly more lateralization than WT (**Fig. 3F**), meaning that they used a procedural strategy to learn the position of the food reward rather than using spatial cues like WT mice. Interestingly, *Cntnap2* KO mice had quicker decision times than WT **(Fig. 3G)**. While WT mice demonstrated a longer time to enter a non-baited arm compared to a baited arm, *Cntnap2* KO mice had similar latencies whatever their responses. This was particularly evident for trials with the same pair presented twice back-to-back, allowing mice to consciously remember the exploration **(Fig. 3I-J)**. Together, this suggests a pre-cognition of decision outcomes in WT that is not demonstrated in *Cntnap2* KO mice. Moreover, these quicker decision times are in line with the well-demonstrated impulsiveness in ASD (DSM-5), and suggest an alteration in the spatial representation of reward information. Altogether, we show that *Cntnap2* KO mice present with a lack of declarative memory flexibility, stemming from the use of a procedural learning strategy which biases the acquisition stage towards an altered spatial representation of the environment.

Shift towards striatum-centered activities in *Cntnap2* KO mice

Each learning strategy is known to depend on partially distinct brain systems: hippocampus-dependent supporting spatial learning, or striatum-based leading to procedural learning (White & McDonald, 2002). To assess the learning-induced activity of these different structures, we quantified the levels of the cellular activity marker cFos in structures involved in memory (dorsal hippocampus (dCA1, dCA2, dCA3, dorsal dentate gyrus (dDG); dorso-medial (DMS)

and dorso-lateral striatum (DLS); Prefrontal cortex (infralimbic (IL)), prelimbic (PrL), and anterior cingular (ACC)) at day 3 of the MariEtxa maze task **(Fig. 4A)**. As previously shown, we found a significant activation of dCA1 in trained WT mice compared to naïve controls, consistent with the use of an allocentric/spatial learning strategy (White & McDonald, 2002) **(Fig. 4B)**. In contrast, there was a lack of learning-induced dCA1 activation in the *Cntnap2* KO mice, combined with the hypoactivation of dCA3 compared to WT. This lack of hippocampal activation likely underlies the deficit in temporal binding and spatial learning capabilities in this task **(Fig. 3C)**. Moreover, *Cntnap2* KO mice displayed a significantly higher activation in the DMS with training, that was not replicated in the WT mice **(Fig. 4B)**. No other significant changes were seen in any of the other prefrontal cortex structures measured (DLS, IL, PrL, ACC; **Fig. 4C)**. Together, this supports the central involvement of the DMS to the egocentric learning strategy of *Cntnap2* KO mice.

To further dissect the balance between memory system we analyzed the weight of each structure within the total activation of the system (**Fig. 4E-F**). After training, we found a disproportionate representation of the PFC and striatum structures over the hippocampus in *Cntnap2* KO mice compared to WT (**Fig. 4E**). Indeed, in WT the weight of the activity of the dCA1 was increased in trained mice, likely supporting temporal binding and flexible declarative memory. In contrast, no reorganization of the activity balance was observed in *Cntnap2* KO mice (**Fig. 4F**). Differences in the weight of each sub-structures in trained WT vs *Cntnap2* KO mice affected the dCA1, dCA2, and dCA3, in favor of DMS, IL, and ACC. Overall, we found a compensatory activation of the frontal-striatal structures concomitant with hippocampal hypoactivation. The lack of dCA1 activation likely prevents the generation of fine-tuned temporal integration of discontiguous events leading to flexibility deficits (Chang & Gold, 2003; Etchamendy et al., 2003; Mingaud et al., 2007; Sellami et al., 2017).

In addition to the learning-induced activity of single structures, the between structure pair-wise correlation of activity deepens the understanding of network-wide synchronization. While WT naïve mice presented with mainly positive correlations between the striatum, PFC, and hippocampus, aside from the dDG being negatively correlated with the PFC, *Cntnap2* KO mice displayed mainly negative correlations (**Fig. 4G**). This indicates that, by default, the between-structure relationships are dysregulated in *Cntnap2* KO mice, preventing the use of a hippocampus-based learning strategy. Altogether, the analysis of learning-induced brain activity demonstrates a shift towards a striatum-centered connectivity in *Cntnap2* KO mice, likely to lead to an egocentric learning strategy causing inflexible memory.

Discussion

This study delves into the qualitative changes in memory processing in the *Cntnap2* KO mouse model of autism, revealing that compromised CA1 hippocampal activity disrupts temporal binding capabilities and supports deficits in episodic memory. Additionally, we found that hippocampal dysfunction in *Cntnap2* KO mice shifts the brain's focus toward egocentric learning and enhances striatum-dependent lateralized learning strategy.

Interplay between hippocampus and striatum in memory deficits in the *Cntnap2* KO mice.

Atypicalities in declarative memory have been reported in ASD, with specific impairments in relating items (Minor et al., 2023). Here we demonstrate that the altered relational processing is due to the reduced capacity to temporally bind items together. *Cntnap2* KO mice showed intact temporal binding with short, but not long, time intervals compared to WT mice. Integration of stimuli in time relies on the activity of the hippocampus, in particular of dCA1 (Buzsáki & Tingley, 2018; Chowdhury et al., 2005; Sellami et al., 2017; Tsien et al., 1996). Consistently, we found an impaired activation of the dCA1 and the dCA3 in *Cntnap2* KO mice during the acquisition of the R/DM task (**Fig. 4B**). Moreover, analysis of the activity of broader memory systems during encoding revealed an aberrant activation of the DMS in the *Cntnap2* KO mice, paired with an altered pair-wise correlation between activation of related brain regions (**Fig. 4G**). Indeed, as opposed to the positive correlations observed in WT mice, we found a negative correlation between the DLS, the prefrontal cortex and hippocampus in *Cntnap2* KO mice. This profile was found in naïve groups, suggesting that the bias towards lateralized learning strategy stems from baseline mistuning of the functional connectivity between brain structures necessary for spatial learning in ASD. This shift towards a striatum-centered system also implies a predominance of an unconscious encoding, in which relations between items are learnt via stimulus response, leading to inflexible goal-directed actions, resemblant of habits (Ferbinteanu, 2016).

This was further supported by analyzing the decision times during the encoding stage of the R/DM, which were significantly longer for successful trials in WT mice **(Fig. 3G)**. This implies a pre-cognition of the reward location in WT mice, but not in *Cntnap2* KO mice, consistent with an overuse of procedural systems over spatial, conscious systems. As previously demonstrated (Al Abed, Sellami, et al., 2020; Sellami et al., 2017), dCA1 optogenetic activation only during time intervals only increases temporal binding capacity which in turn rescues R/DM formation. Delineating the associated connectomes would provide an avenue for targeted brain circuit therapy (Hollunder et al., 2024). We therefore posit that dCA1 constitutes a target

to alleviate the cognitive atypicalities in ASD. On a cellular level, the lack of active cells in the dCA1 during acquisition of the task could imply an allocation of the memory trace of the reward location within the striatum, instead of the hippocampus (Rashid et al., 2016). Further experiments are needed to determine whether engram allocation is linked to learning strategies.

Decoding spatial, and temporal maps in autism.

The CA1 region works with other hippocampal areas to form and maintain spatial, temporal and social maps, which are mental representations of our environment. CA1 neurons contribute to encoding and recalling spatial information, enabling individuals to navigate and understand their surroundings. Specific "time cells" create a temporal framework that supports episodic memory, encoding of the passage of time and the prediction of future events (Eichenbaum, 2014). Recent research also suggests that CA1 plays a role in social cognition via so-called "social maps" to process and recall social information that is essential for effective social behaviour and social dynamics (Zhang et al., 2022). There is limited information on how cognitive deficits in ASD evolve over time and their long-term effects in autism. It would be of interest to further address how specific maps are formed and maintained in this condition.

The role of dCA1 in spatial representations has been profusely documented. Consistently, we recently demonstrated the central role of dCA1 in the maladaptive contextual encoding in post-traumatic stress disorder (PTSD), i.e., the degradation of declarative memory surrounding a highly stressful event (Al Abed, Ducourneau, et al., 2020; Brewin, 2011; DSM-5 & Association American Psychiatric, 2013). Interestingly, growing evidence reports the propensity to develop PTSD in ASD (Al Abed et al., 2024; Rumball et al., 2020), suggesting that the lack of dCA1 activation impacts cognition beyond everyday learning. Together, these studies further elaborate on the crucial role of the hippocampus as a promising target to alleviate ASD pathophysiology.

A recent study reports that memory allocation depends on decreased cell activity when freezing behavior starts (Mocle et al., 2024). In the same line, we found that whilst control mice displayed sustained hippocampal activity during memory trace (**Fig. 2J, L**), hippocampus-dependent memory systems were not similarly activated in the *Cntnap2* KO mice (**Fig. 4B; Fig. 2J, L**). Fiber photometry recordings in the dCA1 indicated that deficits in temporal binding and declarative memory originate from a decrease in hippocampal neuronal synchronization and encoding (i.e., amplitude of the calcium transients largely decreased (**Fig. 2**), some peaks of activation absent (*e.g.* 6 sec post sound), and calcium transients no longer correlated with freezing behavior). However, our experimental conditions did not allow to obtain single-cell

resolution for the analysis as in Mocle et al., 2024. Nevertheless, we found that hippocampus-dependent memory systems were not activable in the *Cntnap2* KO mice, contrary to control mice which displayed sustained hippocampal activity during memory trace (**Fig. 2L**). To note, this investigation has been conducted in only one model of ASD, the *Cntnap2* KO. Further studies will have to assess these aspects in different models to fully comprehend the common cognitive mechanisms at play in autism.

Aging-like performance suggests early cognitive decline in autism

We found that *Cntnap2* KO mice present with a deficit in the flexible component of relational/declarative memory, secondary to a reduction of temporal binding capabilities and the use of a procedural learning strategy. Interestingly, this memory profile replicates that of aged wildtype mice (Al Abed, Sellami, et al., 2020; Marighetto et al., 2011; Sellami et al., 2017) and humans (Etchamendy et al., 2012; Sellami et al., 2017). Not only do aged mice demonstrate a deficit of flexibility in the relational/declarative radial maze task when challenged with high demands in temporal binding, but they also display a striatum-biased learning strategy. In line with recent reports in human suggesting that autism represents a risk factor for early cognitive aging (Lecouvey et al., 2015), further investigations are required to determine whether ASD is linked with defined pathological cognitive aging trajectory.

Methods

Mice

3 to 5-month-old naive mice were collectively housed in standard Makrolon cages, in a temperature- and humidity-controlled room under a 12h light/dark cycle (lights on at 07:00), with *ad libitum* access to food and water. We used both males and females to minimize the number of mice produced in this study. WT and *Cntnap2*$^{-/-}$ KO mice (Jackson ID: #017482 (Peñagarikano et al., 2011)) were non-littermates, derived from breeders of the same colony and used for behavior and histological analyses.

All experiments took place during the light phase. We replicated the behavioral experiments in two to four different batches. Every effort was made to minimize the number of animals used and their suffering. All procedures were conducted in accordance with the European Directive for the care and use of laboratory animals (2010-63-EU) and the animals care guidelines issued by the animal experimental committee of Bordeaux University (CCEA50, agreement number A33-063-099; authorization N°21248), and from the Australian National University Animal Experimentation Ethics Committee (protocol numbers A2018/66, A2020/26, and A2021/43).

Trace fear conditioning task (TFC)

Apparatus: Fear conditioning behavior was performed in a Plexiglas conditioning chamber (20 x 20 x 30 cm), in a brightness of 100 lux, given access to the different visual-spatial cues in the experimental room. The floor of the chamber consisted of stainless-steel rods connected to a shock generator (Imetronic, Pessac, France).

Trace fear conditioning procedure: The box was cleaned with 70% ethanol before each trial.

During acquisition of conditioning, each animal received 3 pairings of a tone (70 dB, 1 kHz, 30 s) and a footshock (0.3 mA, 50 Hz, 1 s). The two stimuli were separated by a trace interval of 5, 20, 40 or 60 sec, depending of the group.

All mice were submitted 24 hour later to the *Tone retention test* during which they were re-exposed to the tone alone in a dark and modified chamber [2min pre-tone, 2min tone and 2min post-tone]. A context test was also performed 2 hours later, during which mice were re-exposed to the conditioning chamber alone during 6 min.

Animals were continuously recorded for off-line scoring of freezing, by an experimenter ignorant of the experimental condition/group. Freezing is defined as a lack of all movement except for respiratory-related movements. Acquisition of the TFC was measured by the progression of freezing during the tone across the 3 tone deliveries. 24h-retention of the trace association was measured during the tone test by the evolution of percentage of freezing time.

Radial-maze task of (Relational/) Declarative memory (DM)

Apparatus: We used an open 8-arm radial maze made of grey Plexiglas, automatized by videotracking (IMETRONIC – Pessac, France). The diameter of the central platform is 30 cm and the arms are 55 cm long by 10 cm large. Each arm is equipped with a door at its entrance and a food-pellet delivering system at its end. The doors are individually controlled (raised up or dropped down) by the computerized system which also controls pellets availability in the food tray at the end of each arm individually, according to the task. The maze is placed in an empty room containing visual cues to enable spatial discrimination.

Behavioral Procedure: During the entire procedure, animals were submitted to one daily session. Prior to memory testing, animals were habituated to the apparatus over a period of two days during which animals were allowed to move freely in the radial maze. To complete the session, mice had to visit each arm until its end. Choice accuracy was measured as the percentage of correct responses for each pair.

Stage 1: Acquisition of 3-pair discriminations

The acquisition task consisted in learning the position of the food within the maze. Indeed, each animal was assigned three adjacent pairs of arms (pairs A, B and C). In each pair, only one arm was baited as a food reward. The experiment is designed in a way that the left arms of the pairs A and B are baited while the right arm of the pair C is. In each trial, mice were given access to a pair (either pairs A, B and C). A choice was considered to be made when the subject had reached the food well of an arm; this also closed the door of the non-chosen arm. The trial was finished as soon as the animal returned to the central platform. The subject was then confined to the central platform for 20s before the next discrimination trial began: this constituted the inter-pair interval. Each daily session consisted of 20 consecutive trials comprising alternate presentations of pairs A, B and C according to a pseudo-random sequence.

A mouse was considered to reach criterion when its overall choice accuracy was at or above 75% over two consecutive sessions given that performance in each of the three discrimination choices were at least 62% correct. The test task began the following day when criterion performance was reached.

Stage 2: Flexibility probe of DM

In the test task, the position of the food in the maze did not change, but characteristic flexibility of DM expression was assessed by changing the way of presenting the arms. Indeed, in place of the pairs A and B, a pair AB was submitted to the mouse. The AB pair consisted in the combination of the two adjacent arms of the pairs A and B. It was the critical test of flexibility. Two other pairs were used as control: the pair C that remained unchanged ("unchanged learnt control", and pair N (=new) made of the two arms non-used in acquisition ("unlearnt control").

FiberPhotometry. *Surgery:* Mice were injected unilaterally 4 weeks before behavioral experiments with an Adeno-Associated Virus (AAV) GCaMP6f (AAV1-hsyn- jGCaMP6f-

WPRE, Addgene). We used glass pipettes (tip diameter 25-35 μm) connected to a picospritzer (Parker Hannifin Corporation) into the right side of the dorsal CA1 of the hippocampus (0.1 μl/site; AP -1.8 mm; L +1.35 mm; DV -1.4 mm). Mice were then implanted with unilateral optic fiber implant (diameter: 200μm; numerical aperture: 0.39; flat tip; Neurophotometrics). Implants were fixed to the skull with Super-Bond dental cement (Sun Medical, Shiga, Japan). Mice were perfused after experiments to confirm correct placements of fibers (**Fig. S4c-e, g**). Viral injections targeted the pyramidal cell layer of the dCA1.

Recordings: Data were recorded using a Neurophotometrics FP3002 system (Neurophotometrics, San Diego, CA). Briefly, 470 and 415 nm LED light was bandpass filtered, reflected by a dichroic mirror, and focused onto a multi-branch patch cord (Neurophotometrics, San Diego, CA) by a x20 objective lens. Alternating pulses of 470 and 415 nm light (~50 μW) were delivered at 60 Hz, and photometry signals were time-locked to behavior using a Bonsai workflow. Signals were analyzed using the Synaptech suite cloud service (MetaCell) and custom-made Python scripts (Code available at https://github.com/elisecr/fiberphotometry_2024). Through the Synaptech platform, 470 and 415 signals were deinterleaved. For all experiments except context and tone test, the exponential delay period (the first 10 seconds REF) of the recording were removed. To correct for photobleaching, isosbestic (415nm) signals were fit to a biexponential curve to model the baseline signal with photobleaching. The fitted biexponential curve was then scaled to match the 470nm signal using non-negative robust linear regress, and subtracted from the 470 trace to correct for baseline drift. Traces were then Z scored.

Experimental traces: Z scored data were analysed by custom-built python scripts to create traces for each experiment. For the trace fear conditioning experiments, these data were aligned to files generated by the Imetronic .dat files to align the beginning of the tone and shock events to the closest millisecond in the Z scored data. These were then extracted to provide traces for each event of interest. For the context and tone test, the first 10 seconds of the experiment was also represented in the trace. For the tone test, the timing of the tone was extracted as described above to accurately align the data.

Peak finding: The threshold for peak analysis definition was set at 1.0. Peak analysis was conducted using a custom-built Python script to calculate peak frequency and amplitude.

Behaviour analysis: Timestamps of behavior of interest for each experiment, including freezing, were manually coded during the experiment. Through the synaptech platform, these were then aligned to this Z scored data to provide bouts of behavior. These bouts were defined by a minimum separation of 0.5s and minimum duration of 0.3s. Bouts of digging and grooming were then extracted by custom built python scripts to quantify the duration of each behavior

over relevant experiments. Bouts of interaction with object and mouse in social preference experiments were also quantified as previously described. In the Synaptech pipeline, defined bouts were then analyzed for the area under the curve (AUC) and mean for 10 seconds before, during and 40 seconds after bouts. Custom-built Python scripts were created to average and display these data.

Code available at https://github.com/elisecr/fiberphotometry_2024

Immunohistochemistry. Animals were perfused transcardially 90 min after the flexibility test on Day 3 for c-Fos analysis with 0.01M phosphate buffered saline (PBS) to eliminate blood and extraneous material, followed by 4% paraformaldehyde (PFA). Brains were postfixed for 36h in PFA. Tissues were sectioned at 40 µm using a Leica 1000S vibratome and kept in a cryoprotective ethylene glycol solution at -20˚C until processed for immunofluorescence. Sections were first washed and permeabilized in PBS-Triton 0.25%, then non-specific binding sites were blocked by immersing the tissue in 10% normal donkey serum, 2% bovine serum albumin in PBS-Triton 0.25% during 2h. Tissues were then stained using the primary antibodies overnight: mouse anti-c-Fos (1:1000; Santa Cruz). After 3x 15 min washes, we added anti-rabbit Alexa 488 (1:200; Life Technologies) secondary antibodies for 2h. After 3x 15 min washes slices were stained during 5 min with DAPI (5µM; Sigma), mounted on Livingstone slides then covered with Mowiol (Sigma) and coverslip (Thermofisher). c-Fos, staining from 2-3 slices par animals were imaged using a Nikon Axioscan confocal fluorescent microscope (20x objective). Stained sections of control and mutant mice were imaged during the same imaging session. Immunofluorescence signals were quantified using the quPath software with routine particle analysis procedures (size= 30-500; circularity=0.30-1.00), to obtain nuclear masks, divided by the area to obtain cell density per mm^2.

Statistics. Data are presented as mean ± SEM. Statistical analyses were performed using GraphPad prism or StatView software for 2-way ANOVA, followed by Bonferroni *post-hoc* test or Student's t test, when appropriate. Normality of the data was confirmed using the Kolmogorov–Smirnov test. Statistical significance was considered at $p<0.05$.

Data availability

All data are available in the main text. Raw data will be made available upon reasonable request. Code available at https://github.com/elisecr/fiberphotometry_2024

Acknowledgments

We thank all the personnel of The Australian Phenomics Facility and of The Neurocentre Magendie involved in mouse care.

Funding

Australian National University Futures scheme, NHMRC Ideas Grant 2019416, Centre National pour la recherche scientifique (CNRS), Bordeaux University, L'institut national de la santé et de la recherche médicale (INSERM), the John Curtin School of Medical Research.

Author contributions

Conceptualization: ASA;

Methodology: ASA, ND, AM, MHM;

Investigation: ASA, ECR

Writing—original draft: ASA, ND

Writing—review & editing: ND, ASA, AM, ECR

Competing interests

Authors declare that they have no competing interests.

Figures and Legends

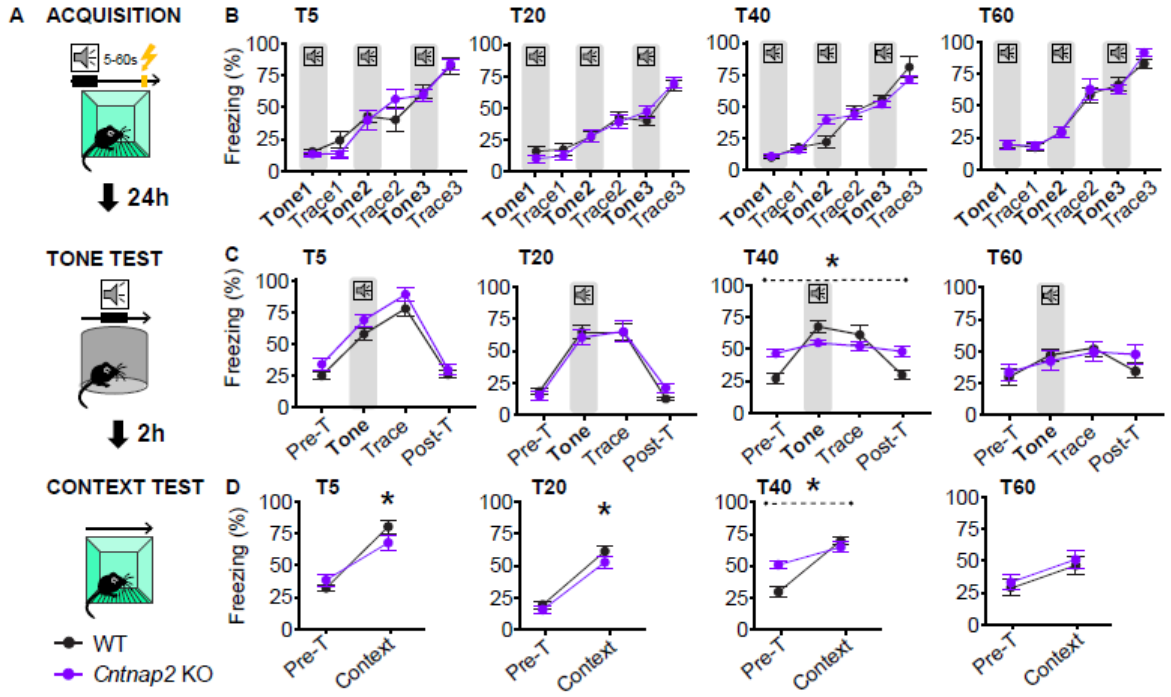

Figure 1. *Cntnap2* KO display reduced temporal binding capabilities

A. Experimental design: Trace Fear Conditioning includes a conditioning session in which mice have to associate a tone and a shock, separate by a time interval (trace). Independent groups of mice were trained with trace intervals of 5, 20, 40, or 60 seconds. **B.** Freezing levels (percent) during acquisition for WT (black) and *Cntnap2* KO (purple) groups, conditioned with distinct trace durations. **C.** Freezing levels (percent) during the tone test for WT (black) and *Cntnap2* KO (purple) groups, 24h post-conditioning with distinct trace durations. **D.** Freezing levels (percent) during the context test for WT (black) and *Cntnap2* KO (purple) groups, 24h post-conditioning with distinct trace durations.

Data shown at mean ± SEM. *: $p<0.05$; **: $p<0.01$; # shows genotype x performance interaction.

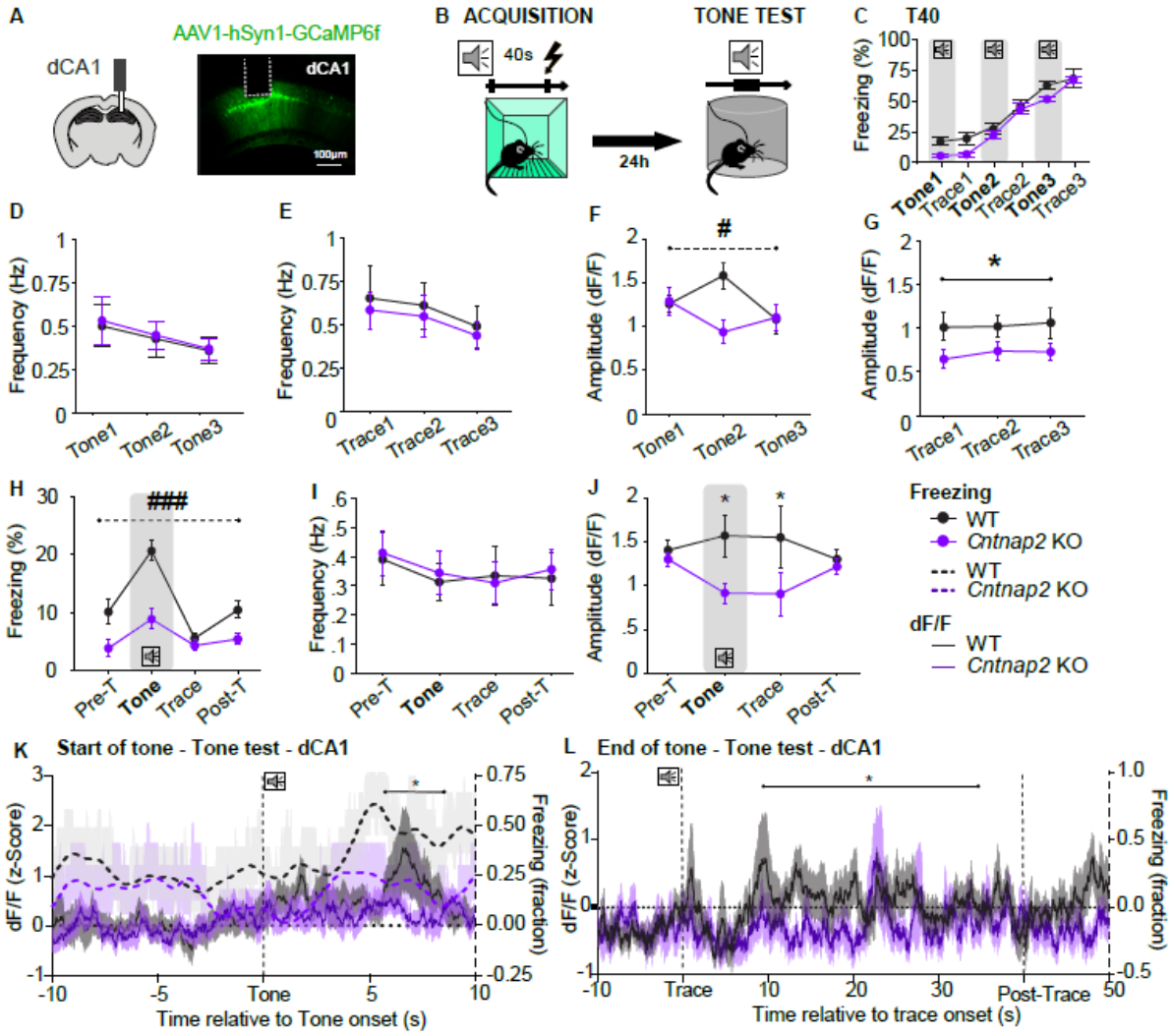

Figure 2. Altered calcium responses during fear conditioning and recall in *Cntnap2* KO

A. Left panel: scheme depicting the fiber optic implantation targeting the dorsal CA1 subfield of the hippocampus (dCA1). Right panel: Representative image of the optic fiber placement, in the pyramidal cell layer of the dCA1, scale: 100µm. Calcium activity was recorded using the calcium indicator GCaMP6f. **B.** Experimental design: Mice were trained in the Trace Fear Conditioning paradigm under a 40s trace interval, followed by a tone test 24h later. **C.** Freezing levels (percent) during acquisition for WT (black) and *Cntnap2* KO (purple) groups, conditioned with a 40s trace interval (T40). **D.** peak frequency of Ca^{2+} transients during the 3 tone presentations of the conditioning (ns). **E.** peak frequency of Ca^{2+} transients during the 3 trace intervals of the conditioning (ns). **F.** peak amplitude of Ca^{2+} transients during the 3 tone presentations of the conditioning (Genotype x Tone interaction: p=0.0247; WT n=11; KO n=10). **G.** peak amplitude of Ca^{2+} transients during the 3 trace intervals of the conditioning (Genotype: p=0.0408; WT n=11; KO n=10). **H.** Freezing levels (percent) during the tone test

for WT (black) and *Cntnap2* KO (purple) groups, 24h post-conditioning (Genotype x Tone interaction: p=0.0007; WT n=11; KO n=10). **I.** Peak frequency of Ca^{2+} transients across the tone test (ns). **J.** Peak amplitude of Ca^{2+} transients across the tone test. **K.** Tone test: comparison between freezing and dCA1 responses relative to tone onset. **L.** Tone test: comparison between freezing and dCA1 responses relative to the end of the tone (i.e., trace onset).

Data shown at mean ± SEM. *: p<0.05; **: p<0.01; ***: p<0.001; * represents genotype effect. # represents genotype x tone interaction.

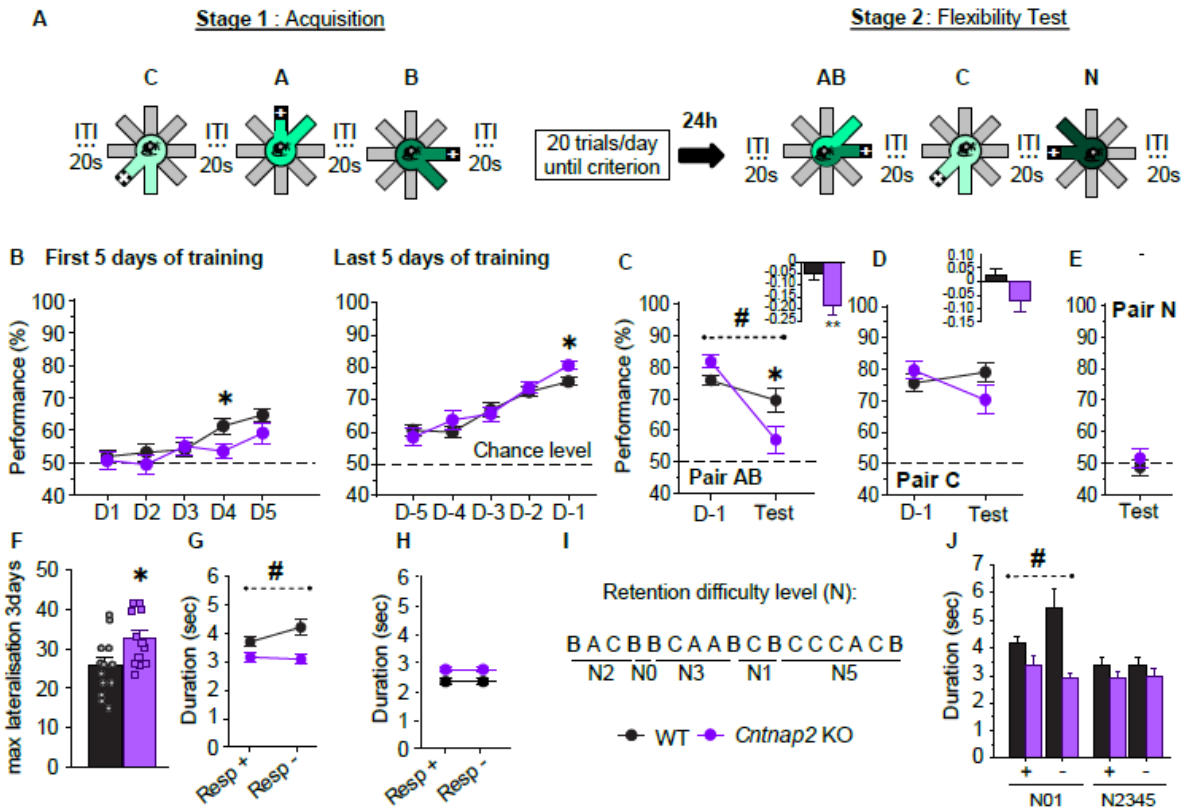

Figure 3. *Cntnap2* KO mice display impaired relational/declarative memory.

A. Experimental design: Relational/Declarative memory task. ITI: Inter-trial interval; +: represent reward location within each pair of arms. **B.** Average correct answers for WT (black; n = 12) and *Cntnap2* KO mice (purple; n = 13) for pairs A, B, and C during the 5 first days of acquisition (left panel; day (D)), and the last 5 days of acquisition (right panel; D-5: 5 days before they reach learning criterion). **C.** Comparison of the correct answers during the last day of training (D-1) averaged on pairs A and B, and during the flexibility test on the recombined pair AB. Inset: D-1 *vs.* Test performance index on pairs AB. **D.** Comparison of the correct

answers on pair C during the last day of training (D-1) and the flexibility test. Inset: D-1 *vs*. Test performance index for Pair C. **E.** Average performance on the new pair N during the flexibility test. **F.** Maximum lateralization index during stage 1 (average performance pairs A and B (left baited) vs Pair C (right baited)). **G.** Average decision latencies for correct (+) and incorrect (-) answers throughout training. **H.** Average runtimes for correct (+) and incorrect (-) answers throughout training. **I.** paradigm: example of pairs presentations sequence and retention difficulty levels, *i.e.,* number of interspaced pairs between 2 presentations of the same pair, here, pair B. **J.** Average decision latencies for correct (+) and incorrect (-) answers depending on the recency of the pair presentation (difficulty levels N) throughout training.

Dashed line illustrates chance level. Data shown at mean ± SEM. *: p<0.05; **: p<0.01; # shows genotype x performance interaction.

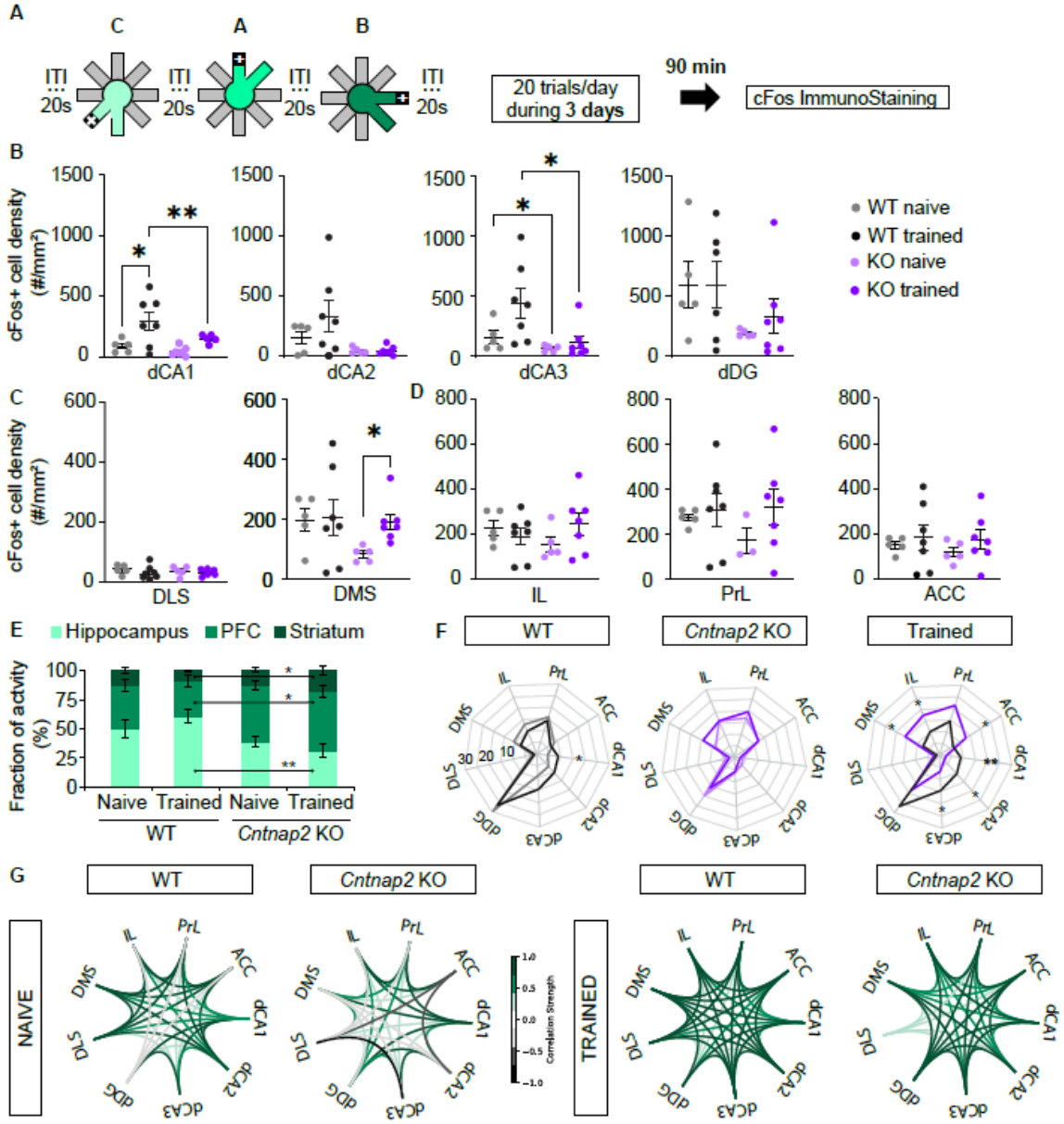

Figure 4. Learning-induced functional connectivity *Cntnap2* KO mice display impaired relational/declarative memory.

A. Experimental design: cFos levels were quantified 90min after the 3rd training session of the Relational/Declarative memory task. ITI: Inter-trial interval; + represent reward location within each pair of arms. **B.** number of cFos-positive neurons (cell density/mm^2) in the hippocampus subfields: dCA1, dCA2, dCA3, dDG for naïve (light colors) and trained (dark colors) WT (grey/black) and *Cntnap2* KO (purple) groups. **C.** number of cFos-positive neurons (cell density/mm^2) in the striatum: DMS, DLS. **D.** number of cFos-positive neurons (cell density/mm^2) in the prefrontal cortex: IL, PrL, ACC. **E.** Proportion of activity for each structure compared to the total activity measured (percentage). **F.** Weight of the activity each subfield within the total network activity (percentage), in WT mice (naïve vs trained, left panel), in *Cntnap2*KO mice (Naïve vs trained, middle panel), and in trained mice (WT vs *Cntnap2* KO mice, right panel, same data as in left and middle panels). **G.** Pairwise between-structure correlation strength of cFos cell density.

Data shown at mean ± SEM. *: $p<0.05$; **: $p<0.01$; # shows genotype x performance interaction.

Al Abed, A. S., Allen, T. V., Ahmed, N. Y., Sellami, A., Sontani, Y., Rawlinson, E. C., Marighetto, A., Desmedt, A., & Dehorter, N. (2024). Parvalbumin interneuron activity in autism underlies susceptibility to PTSD-like memory formation. *IScience*, *27*(5), 109747. https://doi.org/10.1016/j.isci.2024.109747

Al Abed, A. S., Ducourneau, E.-G., Bouarab, C., Sellami, A., Marighetto, A., & Desmedt, A. (2020). Preventing and treating PTSD-like memory by trauma contextualization. *Nature Communications*, *I*, 1–9. https://doi.org/10.1038/s41467-020-18002-w

Al Abed, A. S., Sellami, A., Potier, M., Ducourneau, E. G., Gerbeaud-Lassau, P., Brayda-Bruno, L., Lamothe, V., Sans, N., Desmedt, A., Vanhoutte, P., Bennetau-Pelissero, C., Trifilieff, P., & Marighetto, A. (2020). Age-related impairment of declarative memory: linking memorization of temporal associations to GluN2B redistribution in dorsal CA1. *Aging Cell*, *April*, 1–12. https://doi.org/10.1111/acel.13243

Bal, V. H., Kim, S. H., Cheong, D., & Lord, C. (2015). Daily living skills in individuals with autism spectrum disorder from 2 to 21 years of age. *Autism*, *19*(7), 774–784. https://doi.org/10.1177/1362361315575840

Banker, S. M., Gu, X., Schiller, D., & Foss-Feig, J. H. (2021). *Hippocampal contributions to social and cognitive deficits in autism spectrum disorder*. https://doi.org/10.1016/j.tins.2021.08.005

Blanchard, R. J., Flannelly, K. J., & Blanchard, D. C. (1986). Defensive behavior of laboratory and wild Rattus norvegicus. *Journal of Comparative Psychology (Washington, D.C. : 1983)*, *100*(2), 101–107. https://doi.org/10.1037/0735-7036.100.2.101

Brewin, C. R. (2011). The Nature and Significance of Memory Disturbance in Posttraumatic Stress Disorder. *Https://Doi.Org/10.1146/Annurev-Clinpsy-032210-104544*, *7*, 203–227. https://doi.org/10.1146/ANNUREV-CLINPSY-032210-104544

Buzsáki, G., & Tingley, D. (2018). Space and Time: The Hippocampus as a Sequence Generator. In *Trends in Cognitive Sciences* (Vol. 22, Issue 10, pp. 853–869). Elsevier Ltd. https://doi.org/10.1016/j.tics.2018.07.006

Chang, Q., & Gold, P. E. (2003). Switching memory systems during learning: changes in patterns of brain acetylcholine release in the hippocampus and striatum in rats. *The Journal of Neuroscience : The Official Journal of the Society for Neuroscience*, *23*(7), 3001–3005. http://www.ncbi.nlm.nih.gov/pubmed/12684487

Chowdhury, N., Quinn, J. J., & Fanselow, M. S. (2005). Dorsal hippocampus involvement in trace fear conditioning with long, but not short, trace intervals in mice. *Behavioral Neuroscience*, *119*(5), 1396–1402. https://doi.org/10.1037/0735-7044.119.5.1396

Cohen, N. J., Poldrack, R. A., & Eichenbaum, H. (1997). Memory for items and memory for relations in the procedural/declarative memory framework. *Memory (Hove, England)*, *5*(1–2), 131–178. https://doi.org/10.1080/741941149

DSM-5, & Association American Psychiatric. (2013). *Diagnostic and statistical manual of mental disorders : DSM-5.* https://doi.org/10.1176/appi.books.9780890425596

Eichenbaum, H. (2004). Hippocampus : Cognitive Processes and Neural Representations that Underlie Declarative Memory The hippocampus serves a critical role in declarative. *Neuron*, *44*, 109–120.

Eichenbaum, H. (2014). Time cells in the hippocampus: a new dimension for mapping memories. *Nature Reviews Neuroscience*, *15*(11), 732–744. https://doi.org/10.1038/nrn3827

Eichenbaum, H. (2017). On the Integration of Space, Time, and Memory. In *Neuron* (Vol. 95, Issue 5, pp. 1007–1018). Cell Press. https://doi.org/10.1016/j.neuron.2017.06.036

Etchamendy, N., Desmedt, A., Cortes-Torrea, C., Marighetto, A., & Jaffard, R. (2003). Hippocampal lesions and discrimination performance of mice in the radial maze: sparing or impairment depending on the representational demands of the task. *Hippocampus*, *13*(2), 197–211. https://doi.org/10.1002/hipo.10055

Etchamendy, N., Konishi, K., Pike, G. B., Marighetto, A., & Bohbot, D. (2012). *Evidence for a Virtual Human Analog of a Rodent Relational Memory Task : A Study of Aging and fMRI in Young Adults*. *880*, 869–880. https://doi.org/10.1002/hipo.20948

Ferbinteanu, J. (2016). Contributions of hippocampus and striatum to memory-guided behavior depend on past experience. *Journal of Neuroscience*, *36*(24), 6459–6470. https://doi.org/10.1523/JNEUROSCI.0840-16.2016

Hollunder, B., Ostrem, J. L., Sahin, I. A., Rajamani, N., Oxenford, S., Butenko, K., Neudorfer, C., Reinhardt, P., Zvarova, P., Polosan, M., Akram, H., Vissani, M., Zhang, C., Sun, B., Navratil, P., Reich, M. M., Volkmann, J., Yeh, F. C., Baldermann, J. C., … Horn, A. (2024). Mapping dysfunctional circuits in the frontal cortex using deep brain stimulation. *Nature Neuroscience*, *27*(3), 573–586. https://doi.org/10.1038/s41593-024-01570-1

Huerta, P. T., Sun, L. D., Wilson, M. A., & Tonegawa, S. (2000). Formation of temporal memory requires NMDA receptors within CA1 pyramidal neurons. *Neuron*, *25*(2), 473–480. http://www.ncbi.nlm.nih.gov/pubmed/10719900

Lecouvey, G., Quinette, P., Kalpouzos, G., Guillery-Girard, B., Bejanin, A., Gonneaud, J., Abbas, A., Viader, F., Eustache, F., & Desgranges, B. (2015). Binding in working memory and frontal lobe in normal aging: Is there any similarity with autism? *Frontiers in Human Neuroscience*, *9*(MAR). https://doi.org/10.3389/fnhum.2015.00090

Maister, L., & Plaisted-Grant, K. C. (2011). Time perception and its relationship to memory Autism Spectrum Conditions. *Developmental Science*, *14*(6), 1311–1322. https://doi.org/10.1111/j.1467-7687.2011.01077.x

Marighetto, A., Etchamendy, N., Touzani, K., Torrea, C. C., Yee, B. K., Rawlins, J. N. P., & Jaffard, R. (1999). Knowing which and knowing what: a potential mouse model for age-related human declarative memory decline. *The European Journal of Neuroscience*, *11*(9), 3312–3322. http://www.ncbi.nlm.nih.gov/pubmed/10510196

Marighetto, Brayda-bruno, & Etchamendy. (2011). *Studying the Impact of Aging on Memory Systems : Contribution of Two Behavioral Models in the Mouse*. https://doi.org/10.1007/7854

Mingaud, F., Le Moine, C., Etchamendy, N., Mormède, C., Jaffard, R., & Marighetto, A. (2007). The hippocampus plays a critical role at encoding discontiguous events for subsequent declarative memory expression in mice. *Hippocampus*, *17*(4), 264–270. https://doi.org/10.1002/hipo.20262

Minor, G. N., Hannula, D. E., Gordon, A., Ragland, J. D., Iosif, A. M., & Solomon, M. (2023). Relational memory weakness in autism despite the use of a controlled encoding task. *Frontiers in Psychology*, *14*. https://doi.org/10.3389/fpsyg.2023.1210259

Mocle, A. J., Ramsaran, A. I., Jacob, A. D., Rashid, A. J., Luchetti, A., Tran, L. M., Richards, B. A., Frankland, P. W., & Josselyn, S. A. (2024). Excitability mediates allocation of pre-configured ensembles to a hippocampal engram supporting contextual conditioned threat in mice. *Neuron*, *112*(9), 1487-1497.e6. https://doi.org/10.1016/J.NEURON.2024.02.007

Peñagarikano, O., Abrahams, B. S., Herman, E. I., Winden, K. D., Gdalyahu, A., Dong, H., Sonnenblick, L. I., Gruver, R., Almajano, J., Bragin, A., Golshani, P., Trachtenberg, J. T., Peles, E., & Geschwind, D. H. (2011). Absence of CNTNAP2 leads to epilepsy, neuronal migration abnormalities, and core autism-related deficits. *Cell*, *147*(1), 235–246. https://doi.org/10.1016/j.cell.2011.08.040

Peñagarikano, O., & Geschwind, D. H. (2012). What does CNTNAP2 reveal about autism spectrum disorder? *Trends in Molecular Medicine*, *18*(3), 156–163. https://doi.org/10.1016/j.molmed.2012.01.003

Rashid, A. J., Yan, C., Mercaldo, V., Hsiang, H.-L., Park, S., Cole, C. J., De Cristofaro, A., Yu, J., Ramakrishnan, C., Lee, S. Y., Deisseroth, K., Frankland, P. W., & Josselyn, S. A. (2016). Competition between engrams influences fear memory formation and recall. *Science*, *353*(6297), 383–387. https://doi.org/10.1126/science.aaf0594

Rumball, F., Happé, F., & Grey, N. (2020). Experience of Trauma and PTSD Symptoms in Autistic Adults: Risk of PTSD Development Following DSM-5 and Non-DSM-5 Traumatic Life Events. *Autism Research*, *13*(12), 2122–2132. https://doi.org/10.1002/AUR.2306

Sellami, A., Al Abed, A. S., Brayda-Bruno, L., Etchamendy, N., Valério, S., Oulé, M., Pantaléon, L., Lamothe, V., Potier, M., Bernard, K., Jabourian, M., Herry, C., Mons, N., Piazza, P.-V., Eichenbaum, H., & Marighetto, A. (2017). Temporal binding function of dorsal CA1 is critical for declarative memory formation. *Proceedings of the National Academy of Sciences of the United States of America*, *114*(38). https://doi.org/10.1073/pnas.1619657114

Simon, D. M., & Wallace, M. T. (2016). Dysfunction of sensory oscillations in Autism Spectrum Disorder. In *Neuroscience and Biobehavioral Reviews* (Vol. 68, pp. 848–861). Elsevier Ltd. https://doi.org/10.1016/j.neubiorev.2016.07.016

Tsien, J. Z., Huerta, P. T., & Tonegawa, S. (1996). *The Essential Role of Hippocampal CA1 NMDA Receptor – Dependent Synaptic Plasticity in Spatial Memory*. *87*, 1327–1338.

Uddin, L. Q., Supekar, K., Lynch, C. J., Cheng, K. M., Odriozola, P., Barth, M. E., Phillips, J., Feinstein, C., Abrams, D. A., & Menon, V. (2015). Brain state differentiation and behavioral inflexibility in autism. *Cerebral Cortex*, *25*(12), 4740–4747. https://doi.org/10.1093/cercor/bhu161

Vogel, D. H. V., Jording, M., Esser, C., Conrad, A., Weiss, P. H., & Vogeley, K. (2022). Temporal binding of social events less pronounced in individuals with Autism Spectrum Disorder. *Scientific Reports*, *12*(1). https://doi.org/10.1038/s41598-022-19309-y

White, N. M., & McDonald, R. J. (2002). Multiple parallel memory systems in the brain of the rat. *Neurobiology of Learning and Memory*, *77*(2), 125–184. https://doi.org/10.1006/nlme.2001.4008

Zhang, L., Chen, P., Schafer, M., Zheng, S., Chen, L., Wang, S., Liang, Q., Qi, Q., Zhang, Y., & Huang, R. (2022). A specific brain network for a social map in the human brain. *Scientific Reports*, *12*(1). https://doi.org/10.1038/s41598-022-05601-4